

## ORIGINAL ARTICLE

## A role for MALT1 activity in Kaposi's sarcoma-associated herpes virus latency and growth of primary effusion lymphoma

L Bonsignore<sup>1</sup>, K Passelli<sup>1</sup>, C Pelzer<sup>1</sup>, M Perroud<sup>1</sup>, A Konrad<sup>2</sup>, M Thureau<sup>2</sup>, M Stürzl<sup>2</sup>, L Dai<sup>3,4</sup>, J Trillo-Tinoco<sup>5</sup>, L Del Valle<sup>5</sup>, Z Qin<sup>3,4</sup> and M Thome<sup>1</sup>

Primary effusion lymphoma (PEL) is an incurable malignancy that develops in immunodeficient patients as a consequence of latent infection of B-cells with Kaposi's sarcoma-associated herpes virus (KSHV). Malignant growth of KSHV-infected B cells requires the activity of the transcription factor nuclear factor (NF)- $\kappa$ B, which controls maintenance of viral latency and suppression of the viral lytic program. Here we show that the KSHV proteins K13 and K15 promote NF- $\kappa$ B activation via the protease mucosa-associated lymphoid tissue lymphoma translocation protein-1 (MALT1), a key driver of NF- $\kappa$ B activation in lymphocytes. Inhibition of the MALT1 protease activity induced a switch from the latent to the lytic stage of viral infection, and led to reduced growth and survival of PEL cell lines *in vitro* and in a xenograft model. These results demonstrate a key role for the proteolytic activity of MALT1 in PEL, and provide a rationale for the pharmacological targeting of MALT1 in PEL therapy.

Leukemia (2017) 31, 614–624; doi:10.1038/leu.2016.239

## INTRODUCTION

Primary effusion lymphoma (PEL) is a rare B-cell malignancy that originates from B cells latently infected with Kaposi's sarcoma-associated herpes virus (KSHV, also known as human herpes virus-8, HHV8). PEL is almost exclusively observed in immunosuppressed patients, such as organ transplant recipients and HIV-1-infected patients.<sup>1</sup> PEL is an aggressive and incurable malignancy, with a median survival of <6 months under standard multi-agent chemotherapy with cyclophosphamide, hydroxydaunorubicin, oncovin and prednisolone (CHOP).<sup>1</sup>

As for other herpesviruses, KSHV can exhibit either a latent (non-productive) or a lytic (productive) life cycle that are characterized by distinct viral gene expression profiles.<sup>2</sup> Cellular oncogenesis by KSHV requires maintenance of the virus in the latent stage, as productive infection leads to lysis and death of the infected cells. Presently available anti-herpes virus drugs target only the lytic stage of virus replication, therefore latently KSHV-infected lymphoma cells are resistant to antiviral agents.<sup>3</sup> A better understanding of the molecular mechanism of KSHV-driven oncogenesis is required to develop new therapeutic strategies, which should combine agents promoting lytic KSHV reactivation from latently infected cells with drugs that block the spreading of the virus, in order to selectively kill PEL cells.<sup>4,5</sup>

Latent KSHV infection of lymphocytes is associated with constitutive activation of the transcription factor nuclear factor (NF)- $\kappa$ B, which actively promotes virus latency and represses lytic replication *in vitro*.<sup>6–8</sup> NF- $\kappa$ B activity is also critical for the growth of KSHV-infected lymphoma cells *in vivo*, as growth of a xenografted PEL is efficiently delayed by treatment of the animals

with Bay-11-7082, an irreversible inhibitor of NF- $\kappa$ B activation.<sup>9,10</sup> Several KSHV gene products that promote NF- $\kappa$ B activation have been identified. These include the anti-apoptotic viral FLIP protein encoded by the viral open reading frame (ORF) K13,<sup>11</sup> and ORF K15 that is structurally and functionally homologous to the NF- $\kappa$ B-inducing latency-associated membrane protein-2A of EBV.<sup>12–14</sup> K13 has been proposed to largely account for the constitutive NF- $\kappa$ B activation and expression of NF- $\kappa$ B target genes such as c-IAP1/2, cFLIP-L and IL-6 in latently infected lymphocytes.<sup>15</sup> A possible contribution of K15 to NF- $\kappa$ B activation during viral latency is supported by its reported expression in latently KSHV-infected B cells,<sup>16</sup> and the observation that K15 induces NF- $\kappa$ B target genes such as c-IAP2, A20 and TRAF1 in primary human B cells when expressed in the context of an EBV mutant expressing K15 instead of the latent EBV gene latency-associated membrane protein-2A.<sup>13</sup>

Biochemical studies have revealed some insights into the molecular mechanisms that control NF- $\kappa$ B activation by K13 and K15. K13 is a cytoplasmic protein that promotes NF- $\kappa$ B activation via its physical interaction with the IKK complex,<sup>17,18</sup> which phosphorylates the NF- $\kappa$ B inhibitor I $\kappa$ B to target it for proteasomal degradation. K15-dependent NF- $\kappa$ B activation requires the tyrosine residue 481 within the putative SH2-binding site YEEVL in the K15 cytoplasmic domain,<sup>12</sup> together with a stretch of membrane-proximal amino acids that recruit the kinase NIK and the IKK complex.<sup>19</sup> It is likely that additional, yet undiscovered mechanisms contribute to K13- and K15-dependent NF- $\kappa$ B activation.

The paracaspase mucosa-associated lymphoid tissue lymphoma translocation protein-1 (MALT1) is a Cys-dependent, Arg-specific

<sup>1</sup>Department of Biochemistry, Center of Immunity and Infection, University of Lausanne, Epalinges, Switzerland; <sup>2</sup>Division of Molecular and Experimental Surgery, University Medical Center Erlangen, Friedrich-Alexander-University Erlangen-Nuremberg, Translational Research Center, CILL Biomedical Research Center, Erlangen, Germany; <sup>3</sup>Department of Microbiology, Immunology & Parasitology, Louisiana State University Health Sciences Center, Louisiana Cancer Research Center, New Orleans, LA, USA; <sup>4</sup>Department of Oncology, Research Center for Translational Medicine and Key Laboratory of Arrhythmias, East Hospital, Tongji University School of Medicine, Shanghai, China and <sup>5</sup>Department of Pathology, Louisiana State University Health Sciences Center, Louisiana State University Health Sciences Center, Louisiana Cancer Research Center, New Orleans, LA, USA. Correspondence: Z Qin, Department of Microbiology, Immunology & Parasitology, Stanley S. Scott Cancer Center, Louisiana State University Health Sciences Center, 1700 Tulane Ave, New Orleans 70112, LA, US or Dr M Thome, Department of Biochemistry, Center of Immunity and Infection, University of Lausanne, CILL Biomedical Research Center, Chemin des Boveresses 155, Epalinges CH-1066, Switzerland.

E-mail: zqin@lsuhsc.edu or Margot.ThomeMiazza@unil.ch

Received 30 March 2016; revised 20 July 2016; accepted 9 August 2016; accepted article preview online 19 August 2016; advance online publication, 16 September 2016

protease that controls antigen receptor-induced NF- $\kappa$ B activation in lymphocytes via both, its scaffold and protease activities. As a scaffold, MALT1 promotes the activation of the IKK complex, most likely via recruitment of the ubiquitin ligase TRAF6<sup>(ref. 20)</sup> and the linear ubiquitination chain assembly complex.<sup>21,22</sup> The protease activity of MALT1 massively enhances the NF- $\kappa$ B response by the cleavage of A20 and RelB, which negatively regulate the canonical NF- $\kappa$ B pathway in lymphocytes.<sup>23,24</sup>

MALT1 was originally identified as a proto-oncogene in B-cell lymphomas of the mucosa-associated lymphoid tissue, in which MALT1 is constitutively activated as a result of chromosomal translocations that lead to MALT1 overexpression or formation of an oncogenic apoptosis inhibitor protein-2-MALT1 fusion protein.<sup>25</sup> Naturally, MALT1 is activated upon antigenic triggering of the B-cell receptor (BCR)/CD79 complex. This initiates a signaling cascade that activates Bruton's tyrosine kinase (BTK) and induces the formation of the CBM signaling complex formed by CARMA1 (also known as CARD11), BCL10 and MALT1, which is required for MALT1 activation.<sup>26</sup> Constitutive MALT1 activity is observed in diffuse large B-cell lymphomas (DLBCL) of the activated B-cell (ABC) subtype,<sup>27,28</sup> which are characterized by chronic BCR-BTK-CBM signaling.<sup>29</sup> Recently, small molecule inhibitors of MALT1 have been developed that efficiently inhibit the growth of ABC DLBCL in xenograft models,<sup>30,31</sup> but whether MALT1 inhibition may also be effective against virally induced tumors with constitutive NF- $\kappa$ B activation has not been explored.

Here, we have identified a key role for MALT1 downstream of the viral NF- $\kappa$ B inducers K13 and K15 of KSHV, and demonstrated that MALT1 activity is critical for viral latency and cellular growth of PEL cells *in vitro* and in a xenograft model. These findings suggest that therapeutic inhibition of MALT1 may be used as a rational strategy to treat PEL by purging the reservoir of latently infected cells driving this malignancy.

## MATERIALS AND METHODS

### Cell culture, cell treatment and reagents

HEK293T cells (a kind gift of the late Jürg Tschopp, UNIL, Lausanne, Switzerland) and BCBL-1 cells (a kind gift of Pascal Meylan, CHUV, Lausanne, Switzerland) were cultured in Dulbecco's Modified Eagle Medium and in RPMI (Roswell Park Memorial institute) 1640, respectively, supplemented with 10% fetal bovine serum and antibiotics. The lymphoma cell lines BC-3, BC-1 and BCP-1 (ATCC) and HBL-1 (a kind gift of Louis Staudt, NCI, Bethesda, MD, USA) were cultured in RPMI 1640 supplemented with 20% fetal bovine serum and antibiotics. Lentivirally transduced HEK293T, BCBL-1 and BC-3 cells were kept under puromycin selection (1  $\mu$ g/ml) at all times. All cell lines were regularly tested for mycoplasma (using MycoAlert Mycoplasma Detection Kit, Lonza, Basel, Switzerland). Thioridazine (Sigma-Aldrich, Buchs, Switzerland), staurosporine (Sigma-Aldrich), and ibrutinib (Selleck Chemicals, Houston, TX, USA) were diluted in phosphate-buffered saline (thioridazine) or dimethyl sulfoxide (all others), and used to treat cells at indicated final concentrations. For KSHV reactivation assays, BCBL-1 and BC-3 cells were resuspended in media containing thioridazine, incubated for 6 h, then spun down and resuspended in fresh RPMI media. RNA was harvested 24 h after onset of thioridazine treatment.

### Quantitative Real Time PCR

Total RNA from BCBL-1 and BC-3 cells was extracted with TRIzol reagent (Life Technologies, Thermo Fisher Scientific, Reinach, Switzerland) according to manufacturer's instructions and complementary DNA was synthesized with a High Capacity cDNA Reverse Transcription kit (Applied Biosystems, Thermo Fisher Scientific). SYBR Green fluorescent reagent and LightCycler480 Real Time PCR System (Roche Diagnostics, Basel, Switzerland) were used for quantitative RT-PCR. The relative amount of mRNA was calculated by the comparative threshold cycle method with the housekeeping gene GAPDH (forward: 5'-GAAGGTGAAGGTCGGAGT-3', reverse: 5'-GAAGATGGTGATGGGA TTTC-3') as control. Primers for ORF57 (forward: 5'-TGGACATTATGAAGGGC ATCC-3', reverse: 5'-CGGGTTCGGACAATTGCT-3') and gB (forward: 5'-TCGCCG ACCAATACCATA-3', reverse: 5'-CCTCGGATCTACGTCGGG-3')<sup>8</sup> and for K8.1 (forward: 5'-TGGTGCTAGTAACCGTGTGCC-3', reverse: 5'-TCTGCATTGTAGTGGC CGTC-3')<sup>32</sup> have been previously described.

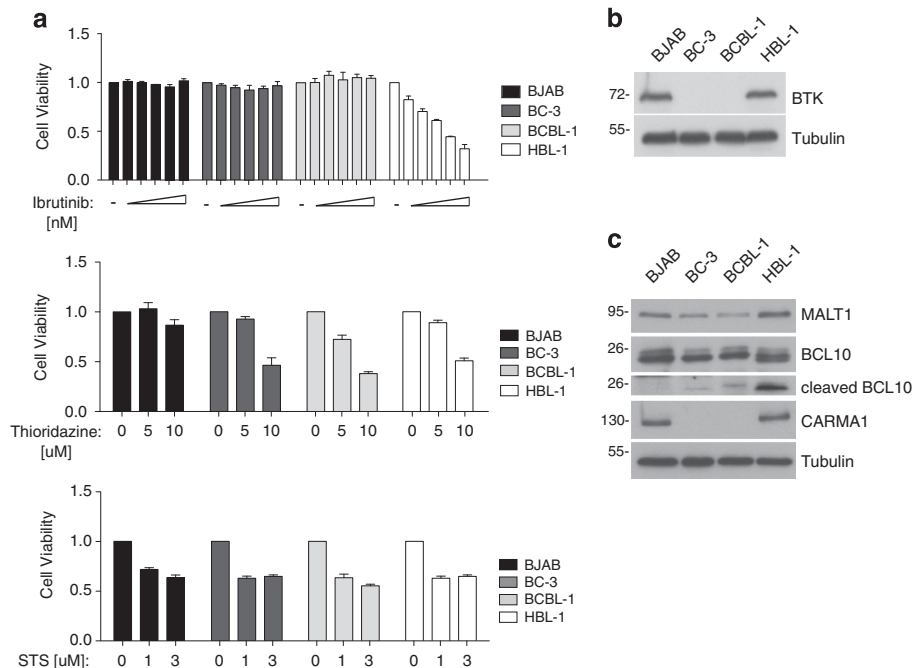


**Figure 1.** MALT1 activity is required for survival of PEL cell lines. **(a)** Cell viability analysis of BJAB (GCB DLBCL), HBL-1 (ABC DLBCL), BC-3 and BCBL-1 (PEL) cells treated with 3.125, 6.25, 12.5, 25 or 50 nM of the BTK inhibitor ibrutinib for 72 h, with the indicated concentrations of the MALT1 inhibitor thioridazine for 48 h, or with staurosporine (STS) for 3 h. **(b)** and **(c)** Western blot analysis of the indicated cell lines to assess expression of BTK **(b)**, or MALT1, BCL10, CARMA1 and cleavage of BCL10 **(c)**. Tubulin blot serves as a loading control. Data are means  $\pm$  s.d. of duplicate (ibrutinib) or triplicate (all others) measurements **(a)** and representative of two independent experiments **(a-c)**.

**KSHV reactivation assays**

HEK293T cells ( $3 \times 10^5$  cells/well) were seeded in a six-well plate, and infected 24 h later with rKSHV219,<sup>33</sup> which expresses green or red fluorescent protein dependent on the latent or lytic viral state, respectively, in the presence of 8  $\mu\text{g}/\text{ml}$  polybrene (S2667, Sigma-Aldrich). On day 2, cells were washed and on day 4, supernatant was harvested and used to infect wild-type HEK293T cells, previously seeded at  $1 \times 10^5$  cells/well in a 12-well plate. On day 7, HEK293T cells were harvested and analyzed by flow cytometry for green fluorescent protein expression.

**Cell viability assay**

Cells ( $2.5 \times 10^5/\text{ml}$ ) were treated with indicated concentrations of thioridazine, staurosporin, ibrutinib or vehicle alone (phosphate-buffered saline or dimethyl sulfoxide) for 48, 3 and 72 h, respectively, and cell viability was assessed using 3-(4,5-dimethylthiazol-2-yl)-5-(3-carboxymethoxyphenyl)-2-(4-sulfophenyl)-2H-tetrazolium (MTS, Promega, Dübendorf, Switzerland, at 400  $\mu\text{g}/\text{ml}$ ) and phenazine methosulfate (PMS, Sigma-Aldrich, at 9  $\mu\text{g}/\text{ml}$ ), according to the manufacturer's instructions. Reduction of MTS to formazan was measured at 492 nm with Capture 96 Software (Basel, Switzerland) on a LEDTECT 96 microplate spectrophotometer (Dynamica Scientific, Zürich, Switzerland). Cell viability of ibrutinib-treated cells was assessed using WST-1 assay (Roche Diagnostics) following the manufacturer's instructions.

**Antibodies**

Antibodies used for western blotting include anti-BTK (D3H5, Cell Signaling Technology/Bioconcept, Allschwil, Switzerland), anti-BCL10 (H197, Santa Cruz Biotechnology/Labforce AG, Muttenz, Switzerland), anti-CARMA1 (1D12, Cell Signaling Technology/Bioconcept), anti-Tubulin (B-5-1-2, Sigma-Aldrich), anti-Strep-HRP (IBA BioTAGnology/Lucerna-Chem AG, Luzern, Switzerland). Affinity-purified antibodies specific for MALT1 and cleaved BCL10 have been previously described.<sup>27,34</sup> A monoclonal antibody directed against the Myc epitope (clone 9E10) was kindly provided by R Iggo (Bordeaux, France). Horseradish peroxidase-coupled goat anti-mouse (115-035-146) and anti-rabbit (111-035-144) were from Jackson ImmunoResearch (Milan Analytica AG, Rheinfelden, Switzerland).

**Protein expression vectors**

Expression vectors for the 86 myc-tagged ORFs of KSHV in a pcDNA4 background have been previously described.<sup>35-37</sup> Point mutants of K13 or K15 expression constructs were generated by quick-change PCR using PfuUltra high-fidelity DNA polymerase AD (Agilent Technologies, Morges, Switzerland) and verified by sequencing. Tagged MALT1 and BCL10 expression constructs<sup>34,38</sup> and the eYFP-Leu-Val-Ser-Arg-eCFP construct<sup>39</sup> have been previously described.

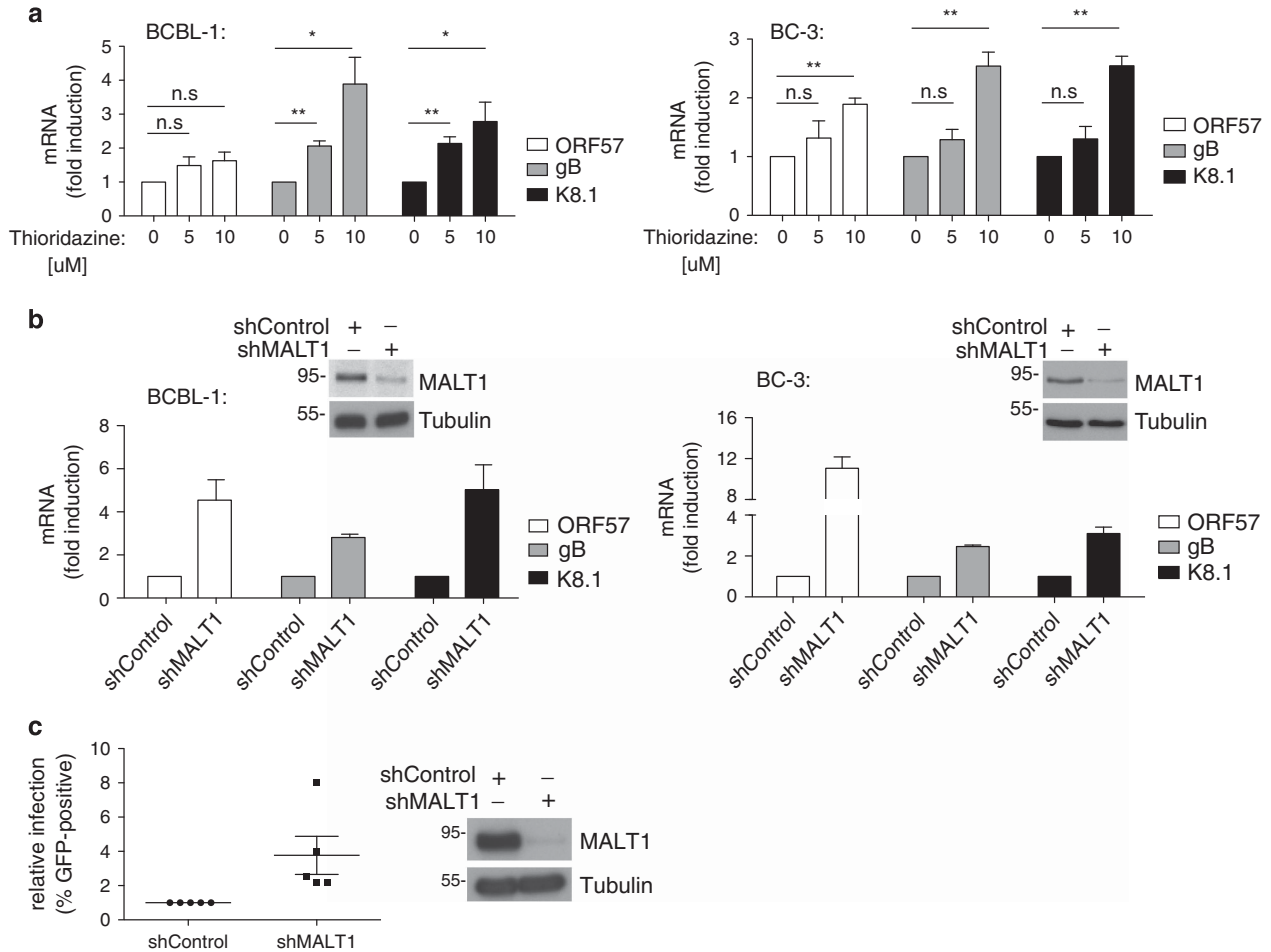


**Figure 2.** MALT1 inhibition promotes KSHV lytic reactivation. (a and b) RT-PCR analysis of the expression of indicated viral lytic genes in BCBL-1 and BC-3 cells treated with vehicle or 5 or 10  $\mu\text{M}$  thioridazine (a), or transduced with MALT1 silencing or control vectors (b). MALT1 protein expression was assessed by western blot. Tubulin blot serves as a loading control. (c) Assessment of production of infectious virus particles by 293 T cells stably transduced with a silencing vector for MALT1 or a control vector, and infected with rKSHV219.<sup>33</sup> MALT1 protein expression in the initial 293 T cell population was monitored by western blot. Tubulin blot serves as a loading control. Data in (a) and (c) represent means ( $\pm$  s.d.) of two (a) or three (c) independent experiments. Data in (b) represent means  $\pm$  s.d. of triplicate measurements, representative of two independent experiments. ns: not significant; \* $P < 0.05$ ; \*\* $P < 0.01$  (unpaired *t*-test).

**Transfection and transduction of cells, gene silencing**

Transient transfection of HEK293T cells and lentiviral transduction of HEK293T, BCBL-1 and BC-3 cells were performed using previously described methods.<sup>34,38</sup> For silencing of MALT1 in HEK293T, BCBL-1 and BC-3 cells, cells were transduced with a lentiviral vector (pAB286.1, a kind gift of R Iggo, Bordeaux, France) containing short harpin RNA sequences specific for BCL10 (5'-GTAGAGAAGACACTGAAGA-3')<sup>38</sup> or MALT1 (5'-GTCA CAGAATTGAGTGATTC-3').<sup>40</sup>

**Cell lysis, immunoprecipitation and immunoblot analysis**

Cells were lysed in lysis buffer containing 50 mM HEPES, pH 7.5, 150 mM NaCl, 1% Triton X-100, protease inhibitors (Complete; Roche Diagnostics) and phosphatase inhibitors (NaF, Na<sub>4</sub>P<sub>2</sub>O<sub>7</sub> and Na<sub>3</sub>VO<sub>4</sub>). For immunoprecipitation, lysates were precleared for 60 min with Sepharose 6B beads (Sigma-Aldrich). StrepTactin Sepharose beads (IBA) were then added to cleared lysates, followed by incubation for 2 h at 4 °C. Beads were washed five

times with Triton 1% lysis buffer. Samples were boiled in reducing sodium dodecyl sulfate sample buffer, separated by sodium dodecyl sulfate-polyacrylamide gel electrophoresis and analyzed by immunoblot as described.<sup>34</sup>

**NF-κB luciferase reporter assay**

Activation of gene transcription was assessed by transient transfection of HEK293T cells with a NF-κB firefly luciferase reporter construct together with a Renilla luciferase vector (phRL-TK). Cells were lysed in passive lysis buffer (Promega) and luciferase activity assessed using dual luciferase assay (Promega) on a TD-20/20 luminometer (Turner Design, Fisher Scientific, Reinach, Switzerland).

**Analysis of MALT1 protease activity by flow cytometry**

Forster resonance energy transfer-based determination of MALT1 protease activity in HEK293T cells was essentially done as described.<sup>39</sup> In brief,

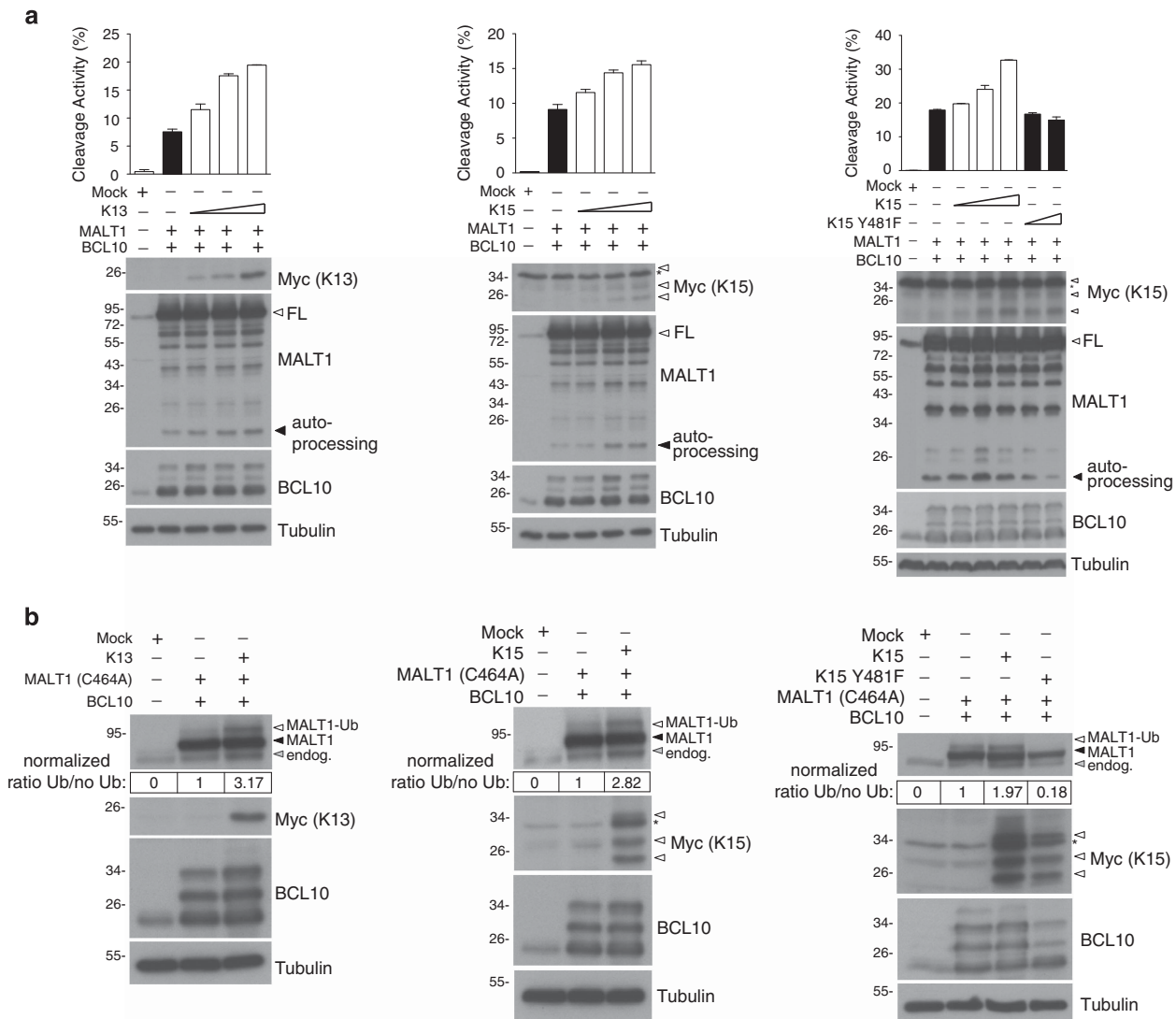


**Figure 3.** K13 and K15 induce MALT1 protease activity. **(a)** 293 T cells were transfected with a eYFP-LVSR-eCFP reporter plasmid and the indicated combinations of expression constructs for MALT1, BCL10, and K13, K15 or the K15 Y481F mutant, and the proportion of cells with MALT1-dependent reporter cleavage was assessed by flow cytometry. Expression of tagged proteins and of MALT1 autoproteolysis was assessed by western blot. Tubulin blot serves as a loading control. Three isoforms are detected for Myc-tagged K15, as previously described.<sup>16</sup> Asterisk indicates a non-specific band detected by anti-Myc. FL, full-length. **(b)** 293 T cells were transfected with the indicated combinations of expression vectors for BCL10 and catalytically inactive MALT1 (C464A), together with K13, K15 or the K15 mutant Y481F, and protein expression and monoubiquitination of MALT1 was monitored by western blot (MALT1-Ub, open arrowhead). The relative increase in MALT1 monoubiquitination by the co-transfected K13 or K15 constructs was quantified by ImageJ. Migration of endogenous (endog., gray arrowhead) and overexpressed MALT1 (MALT1, black arrowhead) isoforms are indicated. Tubulin blot serves as a loading control. Data in **a** represent means ± s.d. of triplicate measurements, and are representative of two independent experiments. Data in **b** are representative of two independent experiments.

HEK293T cells were transfected with the eYFP–Leu–Val–Ser–Arg–eCFP reporter construct, together with indicated combinations of KSHV ORFs, MALT1 and BCL10 expression constructs. After 6 h of transfection, cells were washed and 24 h later resuspended in flow cytometry buffer (2% fetal bovine serum in phosphate-buffered saline) and analyzed with an LSR II flow cytometer (BD Biosciences, Allschwil, Switzerland) containing 405-, 488-, 561- and 640-nm lasers. To measure the eCFP and Förster resonance energy transfer signal, the transfected cells were excited with a standard 450/50 filter for collection of the eCFP fluorescence and a 585/42 filter for Förster resonance energy transfer fluorescence, respectively, and for each sample at least 10 000 highly eYFP+ cells were counted.

**PEL xenograft model**

Aliquots of 10<sup>7</sup> BCBL-1 cells were diluted in 200 µL sterile phosphate-buffered saline, and 6–8 week-old male non-obese diabetic/severe-combined immunodeficiency mice (Jackson Laboratory, Bar Harbor, ME, USA) received intraperitoneal injections with a single-cell aliquot. The MALT1 inhibitors mepazine or thioridazine (10 mg/kg body weight, respectively), or vehicle alone, was administered using an insulin syringe for intraperitoneal injection. Drug was administered either 24 h or 28 days (allowed to establish tumor expansion) after BCBL-1 injection, 3 times/week. Two experiments, with six mice per group for each experiment, were performed. The PEL expansion *in vivo* was confirmed by testing the expression of cell-surface markers including CD45, CD138, EMA and intranuclear expression of the viral protein LANA within ascites tumor cells, using IFA and flow cytometry as described previously.<sup>41</sup> Weights were recorded weekly as a surrogate measure of tumor

progression, and ascites fluid volumes were tabulated for individual mice at the completion of each experiment. Spleen sections were stained by hematoxylin and eosin for identification of tumors infiltrating along vascular channels. Images were collected at ×400 magnification using a Olympus BX61 microscope equipped with a high resolution DP72 camera and CellSense image capture software. All protocols were approved by the Louisiana State University Health Science Center Animal Care and Use Committee in accordance with national guidelines (IACUC, No. 3237).

**Image quantification and statistical analysis**

Quantification of the relative proportion of monoubiquitinated MALT1 in different samples was performed using ImageJ, and signal intensity of monoubiquitinated MALT1 was normalized to the band corresponding to unmodified MALT1. Two-tailed Student's *t*-test was used for statistical analysis.

**RESULTS**

**MALT1 activity is required for survival of PEL cell lines**

An attractive target for the treatment of ABC DLBCL with chronic BCR signaling is BTK, a kinase that acts downstream of the BCR and upstream of the CBM complex.<sup>29</sup> To assess if the survival of PEL cells depends on BTK activity, we treated PEL cell lines BC-3 and BCBL-1 with the BTK inhibitor ibrutinib. As controls, we used HBL-1 cells, which are derived from DLBCL of the ABC type and characterized by constitutive BCR signaling, and BJAB cells, which are derived from

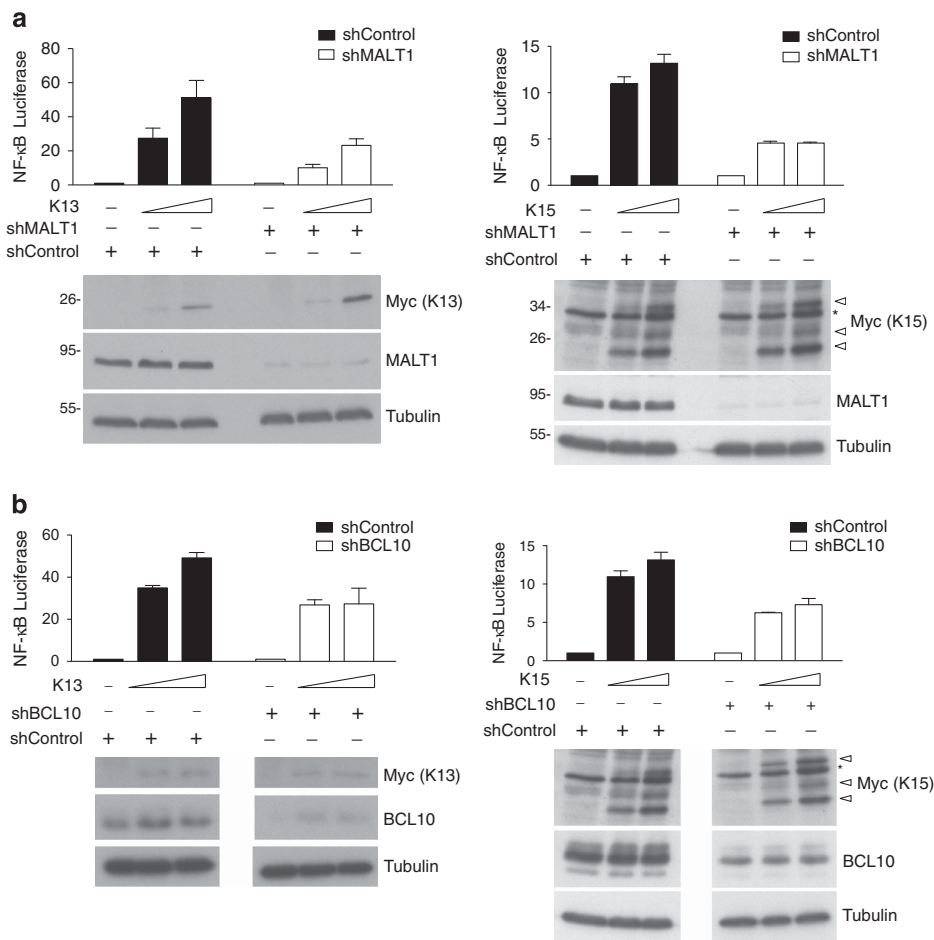


**Figure 4.** K13 and K15 promote NF-κB activation via MALT1. (a and b) 293 T cells stably transfected with silencing constructs for MALT1 (a), BCL10 (b) or a control vector were transfected with increasing concentrations of K13 or K15 and an NF-κB reporter construct, and NF-κB activation was monitored by luciferase assay. Expression of transfected constructs and silencing efficiency was monitored by western blot. Tubulin expression serves as a loading control. Three isoforms are detected for Myc-tagged K15, as previously described.<sup>16</sup> Asterisk indicates a non-specific band detected by anti-Myc. Mock controls for K15 belong to the same experiment in (a) and (b). Data represent means ± s.d. of triplicate measurements, and are representative of two independent experiments.

DLBCL of the GCB subtype in which BCR signaling is not activated.<sup>29</sup> As expected, ibrutinib induced cytotoxicity in HBL-1 cells, but not in BJAB cells. Interestingly, both PEL cell lines were insensitive to BTK inhibition (Figure 1a), and did not express detectable levels of BTK (Figure 1b), whereas BTK expression was easily detectable in the cell lines derived from ABC and GCB DLBCL. Similar results were obtained with two additional PEL cell lines (BC-1 and BCP-1) (Supplementary Figure 1).

Next, we tested whether the CBM complex, and in particular MALT1 activity, might be relevant for PEL cell survival, by treating PEL cell lines with the MALT1 protease inhibitor thioridazine.<sup>30</sup> As expected, MALT1 inhibition led to a clear decrease in cell viability in HBL-1 cells, but did not affect viability of BJAB cells. In addition, the MALT1 inhibitor was cytotoxic for four independent PEL cell lines (Figure 1a, Supplementary Figure 1C). Treatment with the tyrosine kinase inhibitor staurosporine, on the other hand, induced similar cytotoxicity in all lymphoma cell lines

tested (Figure 1a and Supplementary Figure 1D). The thioridazine-induced reduction in cell viability correlated with a dose-dependent induction of apoptotic cell death and caspase-3 processing (Supplementary Figure 1E, see also Supplementary Figure 6C).

Next, we assessed the status of MALT1 expression and activity in the PEL cell lines BC-3 and BCBL-1. Compared with BJAB and HBL-1 cells, PEL cell lines expressed slightly lower levels of MALT1 (Figure 1c and Supplementary Figure 2A). The MALT1-binding protein BCL10 was expressed to similar levels in all lymphoma cell lines tested, but showed a slightly retarded migration pattern in BCBL-1 cells (Figure 1c). MALT1 activity, which can be monitored by the cleavage of BCL10 and by MALT1 autoprocessing,<sup>34,42</sup> was clearly detectable in HBL-1 cells but also, to a lower degree, in the PEL cell lines BC-3 and BCBL-1 (Figure 1c and Supplementary Figure 2B). Treatment with the MALT1 inhibitor thioridazine impaired both BCL10 cleavage and autoprocessing in BCBL-1 cells (Supplementary Figure 2C). We also found evidence for a weak

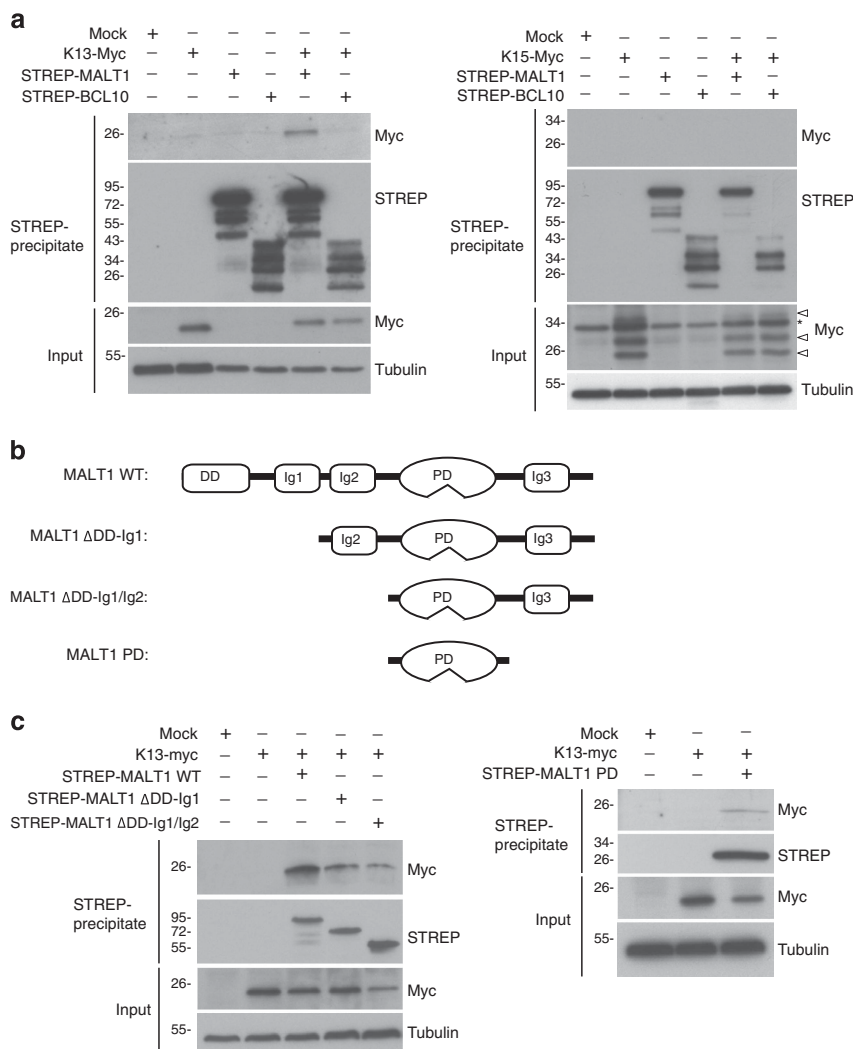


**Figure 5.** K13 but not K15 physically interacts with MALT1. **(a)** 293 T cells were co-transfected with the indicated combinations of tagged expression constructs for MALT1 and BCL10, K13 or K15, and protein expression and binding of K13 or K15 to precipitated MALT1 or BCL10 was monitored by western blot. **(b)** Schematic representation of different MALT1 constructs used to map the MALT1-K13 interaction ( $\Delta$ DD-Ig1, deleted of the DD and first Ig;  $\Delta$ DD-Ig1/Ig2, deleted of the DD and first two Ig domains; PD, protease domain alone). **(c)** 293 T cells were co-transfected with the indicated combinations of tagged expression constructs for K13 and MALT1 ( $\Delta$ DD-Ig;  $\Delta$ DD-Ig1/Ig2; PD), and protein expression and binding of K13 to precipitated MALT1 constructs was monitored by western blot. Tubulin expression serves as a loading control. Three isoforms are detected for Myc-tagged K15, as previously described.<sup>16</sup> Asterisk indicates a non-specific band detected by anti-Myc. Data in all figure panels are representative of two independent experiments.

constitutive cleavage of A20, corresponding to previously described bands of ~65, 55 and 43 kD<sup>23,27</sup> that are detectable with various intensities in the PEL cell lines (Supplementary Figure 2D). Surprisingly, the PEL cell lines did not express CARMA1, a scaffold protein that is essential for antigen receptor-induced MALT1 activation<sup>43,44</sup> (Figure 1c and Supplementary Figure 2A). We also did not detect expression of the CARMA1 homologs CARMA3 (CARD10) and CARD9 (data not shown). Collectively, this suggests that MALT1 activity is essential for the survival of PEL cells, and that MALT1 activation in PEL cells must occur independently of BCR-BTK-CARMA1 signaling.

**Inhibition of MALT1 activity promotes KSHV reactivation in PEL cell lines**

To assess the mechanism underlying PEL cell death upon MALT1 inhibition with thioridazine (Figure 1a), we next monitored the expression of viral lytic genes in the two PEL cell lines BCBL-1 and BC-3. Upon inhibition of MALT1, we observed an increase in the mRNA expression of viral lytic genes such as ORF57 (MTA), gB and K8.1 in two PEL cell lines (Figure 2a). An even stronger effect was obtained upon MALT1 silencing (Figure 2b), which affects both the scaffold and the catalytic function of MALT1. MALT1 silencing also favored the upregulation of the lytic KSHV program and release of infectious virus particles from 293 T cells infected with a previously described recombinant KSHV<sup>33</sup> (Figure 2c). Thus, MALT1 is constitutively active in PEL cell lines, and inhibition of MALT1

activity compromises viral latency and leads to lytic reactivation of KSHV, which specifically drives PEL cell death.

**The latency-associated viral genes K13 and K15 promote MALT1 protease activity**

To identify the mechanisms by which KSHV activates MALT1 in latently infected PEL cells, we screened a validated expression library of 86 ORFs encoded by KSHV<sup>35-37</sup> for their capacity to induce MALT1 protease activity upon co-expression in 293 T cells. For this screen, we made use of a previously established, Forster resonance energy transfer-based reporter assay for MALT1 activity, which is based on the MALT1-dependent cleavage of an eYFP-LVSR-eCFP reporter construct that can be monitored by flow cytometry<sup>39</sup> (Supplementary Figure 3). Among the most potent KSHV genes that increased MALT1 activity were the KSHV-specific genes K13 and K15 (Supplementary Figure 3), which are known as NF-κB-inducing proteins expressed during viral latency<sup>45</sup> (Supplementary Figure 4). When tested individually, both K13 and K15 promoted MALT1 activation in a dose-dependent manner, as evident from reporter cleavage and induction of MALT1 autoprocessing, which is a consequence of MALT1 activation<sup>42</sup> (Figure 3a). K15-induced MALT1 activation was abolished by mutation of Y481 (Figure 3a), a tyrosine residue that is part of an SH2-binding motif required for K15-mediated NF-κB activation<sup>12</sup> (Supplementary Figure 5A). In contrast, mutation of a previously reported TRAF2/3-binding site in K13, which is also

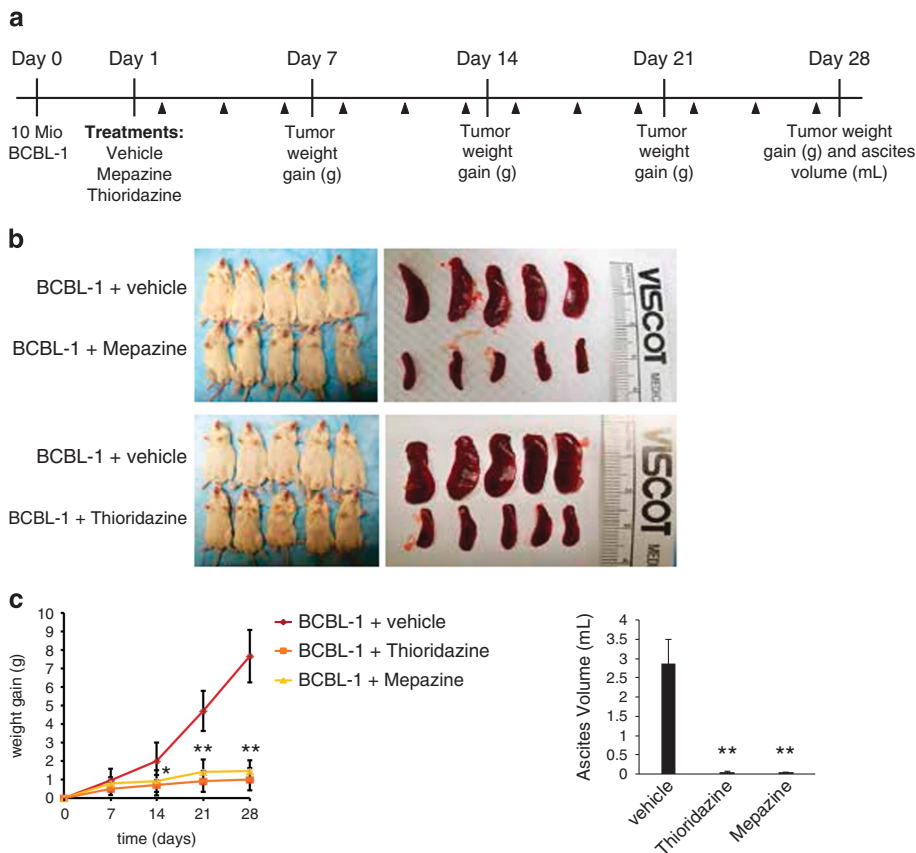


**Figure 6.** MALT1 inhibition prevents growth of PEL in a xenograft model. (a) Overview of the time course of the experiment, indicating time points of injection of PEL cells, treatment and schedule of monitoring. (b) Analysis of the overall size of PEL-injected animals and respective spleens under conditions of treatment with vehicle and either the MALT1 inhibitor mepazine (upper panel) or thioridazine (lower panel). (c) Analysis of the tumor-related gain in body weight (g) or ascites volume (ml) of PEL-injected animals under conditions of treatment with vehicle or the MALT1 inhibitors mepazine or thioridazine. Data shown in (b) represent individual animals (*n* = 5 per group) from one out of two independent experiments. Data in (c) represent means ± s.d. \**P* < 0.01; \*\**P* < 0.001 (unpaired *t*-test).

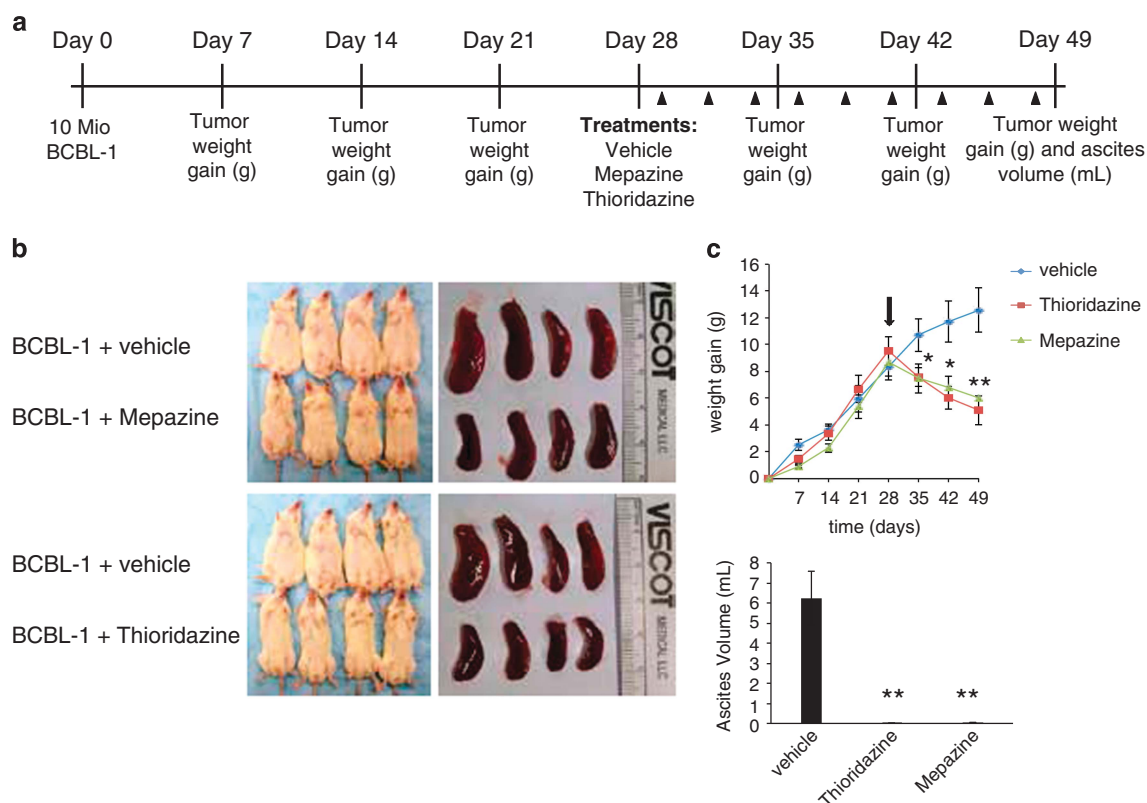


**Figure 7.** MALT1 inhibition leads to regression of established PEL in a xenograft model. **(a)** Overview of the time course of the experiment, indicating time points of injection of PEL cells, start of treatment and schedule of monitoring. **(b)** Analysis of the overall size of PEL-injected animals and respective spleens under conditions of treatment with vehicle and either the MALT1 inhibitor mepazine (upper panel) or thioridazine (lower panel). **(c)** Analysis of the tumor-related gain in body weight (g) or ascites volume (mL) of PEL-injected animals under conditions of treatment with vehicle or the MALT1 inhibitors mepazine or thioridazine. Data shown in **(b)** represent individual animals ( $n=4$  per group) from one out of two independent experiments. Data in **(c)** represent means  $\pm$  s.d. \* $P < 0.01$ ; \*\* $P < 0.001$  (unpaired  $t$ -test).

important for NF-kappa-B essential modulator binding,<sup>46</sup> did not affect the capacity of K13 to activate MALT1 (Supplementary Figure 5B). In activated lymphocytes, optimal MALT1 activation requires its monoubiquitination on K644.<sup>39</sup> Monoubiquitinated MALT1 is stabilized and thus more easily detectable under conditions of catalytic inactivation of MALT1, possibly because of reduced autoprocessing and/or turnover of the active form of MALT1.<sup>39,42</sup> As previously described, co-expression of a catalytically inactive C464A mutant of MALT1 with BCL10 in 293 T cells led to MALT1 monoubiquitination, which can be monitored by the appearance of a slower migrating form of MALT1<sup>(ref.39)</sup> (Figure 3b). Monoubiquitination of MALT1 was further increased by co-expression of K13 or K15 (Figure 3b). K15-induced monoubiquitination of MALT1 was greatly impaired by mutation of Y481 (Figure 3b), consistent with the requirement of Y481 for MALT1 activation (Figure 3a). Collectively, these findings suggest that both KSHV proteins K13 and K15 can induce MALT1 protease activity by promoting the monoubiquitination-dependent activation of MALT1.

K13 and K15-dependent NF-kB activation is impaired upon MALT1 silencing

Next, we tested whether K13 and K15 promote NF-kB gene transcription via MALT1 and possibly via its binding partner BCL10 that is required for MALT1 activation in lymphocytes.<sup>34</sup> Silencing of MALT1 (Figure 4a) or BCL10 (Figure 4b) partially affected both K13- and K15-induced NF-kB activation. Moreover, K13- or K15-induced NF-kB activation was strongly increased by co-expression

of wild-type MALT1, but much less so by the catalytically inactive C464A mutant of MALT1 (Supplementary Figure 6). In addition, we have assessed the effect of the MALT1 inhibitor thioridazine on the expression of the NF-kB target genes cFLIP and c-IAP1, and found that MALT1 inhibition led to a reduced expression of these target genes and a correlating increase in caspase-3 activation (Supplementary Figure 6C). K13 most likely promoted NF-kB activation by direct or indirect physical recruitment of MALT1, as K13 interacted with MALT1 but not with BCL10 upon co-expression of the proteins in 293 T cells (Figure 5a). Under similar conditions, no physical interaction of K15 with MALT1 or BCL10 was detectable (Figure 5a). Using various MALT1 constructs deleted in individual domains (Figure 5b), we then mapped the region of MALT1 that interacted with K13. This revealed that the DD and the two N-terminal Ig domains of MALT1 were not necessary for the interaction, whereas the protease domain was both required and sufficient for the interaction with K13 (Figure 5c). Thus, K13 probably activates MALT1 and consequently NF-kB via binding to its protease domain, either directly or via an additional binding partner. K15 most likely activates MALT1 indirectly, via the Y481-dependent recruitment of additional signaling proteins.

MALT1 inhibitors prevent the growth of PEL in a xenograft model  
To test whether MALT1 inhibition could be of interest for the treatment of PEL, we subsequently assessed the effect of two small molecule inhibitors of MALT1 on the growth of BCBL-1 cells in a xenograft model.<sup>41</sup> BCBL-1 cells were injected



intraperitoneally into non-obese diabetic/severe-combined immunodeficiency mice, and 24 h later, we started treatment of the mice with a 3 times per week intraperitoneal injection of the MALT1 inhibitors mepazine or thioridazine<sup>30</sup> (both at 10 mg/kg) for 4 weeks. Establishment of PEL was monitored by measuring tumor-related gain in body weight, spleen size and ascites volume at the indicated time points (Figure 6a). Compared with mice treated with vehicle alone, mepazine- or thioridazine-treated mice showed an almost complete inhibition of tumor-related gain in body weight and spleen enlargement (Figures 6b and c), and of ascites formation (Figure 6c) measured after 4 weeks of treatment. Hematoxylin and eosin staining enabled us to observe a great amount of tumor infiltration into the spleen of vehicle-treated mice, whereas only small tumor nodules were dispersed in the spleen of mepazine- or thioridazine-treated mice (Supplementary Figure 7). Thus, MALT1 inhibition is highly efficient in preventing the development of xenografted PEL *in vivo*.

MALT1 inhibitors efficiently induces regression of established PEL tumors *in vivo*

Next, we assessed whether MALT1 inhibition was also efficient in mice with already established PEL. To test this, mice were inoculated with BCBL-1 cells at day 0, and treatment with vehicle, mepazine or thioridazine was initiated only after 28 days, when the mice had already well established PEL. Tumor-related gain in body weight, spleen size and ascites volume were monitored at the indicated time points (Figure 7a). Compared with mice treated with vehicle only, mepazine- or thioridazine-treated animals showed a significant regression of tumor-related spleen enlargement and gain in body weight (Figures 7b and c), and a complete loss of measurable ascites volume (Figure 7c) upon 21 days of treatment. Therefore, we conclude that MALT1 inhibition by mepazine or thioridazine is highly efficient not only in preventing

the establishment of PEL expansion, but also in promoting the regression of established PEL in this xenograft model.

## DISCUSSION

In this study, we provide several lines of evidence for an essential role of the paracaspase MALT1 in the malignant growth of latently KSHV-infected PEL cells. First, we found that MALT1 was constitutively active in PEL cell lines in the absence of BCR/BTK/CARMA1 signaling. Second, MALT1 inhibition with a small molecule inhibitor induced the viral lytic program and impaired cell viability. Third, we showed that MALT1 expression and activity contributes to K13- and K15-driven NF- $\kappa$ B activation, which controls the growth and survival of latently KSHV-infected B cells and development of PEL. Finally, MALT1 inhibition prevented the development of xenografted PEL *in vivo*, and led to efficient regression of established PEL in this xenograft model. Collectively, these findings identify MALT1 as a key driver of KSHV latency, and as a potentially interesting target for the treatment of PEL (Figure 8).

Among the latent KSHV genes previously demonstrated to have a capacity to activate NF- $\kappa$ B, K13 and K15 were able to potently promote MALT1 activation. K13 directly or indirectly interacted with MALT1 and in particular its protease domain, and may thus induce a conformational change in the protease domain that promotes MALT1 activation, for example, by rendering it accessible to monoubiquitination. The transmembrane protein K15 seemed to use a distinct mechanism that required Y481 in its cytoplasmic SH2-binding motif, and thus most likely mediates MALT1 activation by the recruitment of an SH2 domain-containing protein that remains to be identified (Figure 8). Both K13 and K15 have previously been described to activate NF- $\kappa$ B via IKK components,<sup>17-19</sup> and MALT1 has been proposed to physically recruit and activate the IKK complex.<sup>20,47</sup> Whether MALT1 and IKK

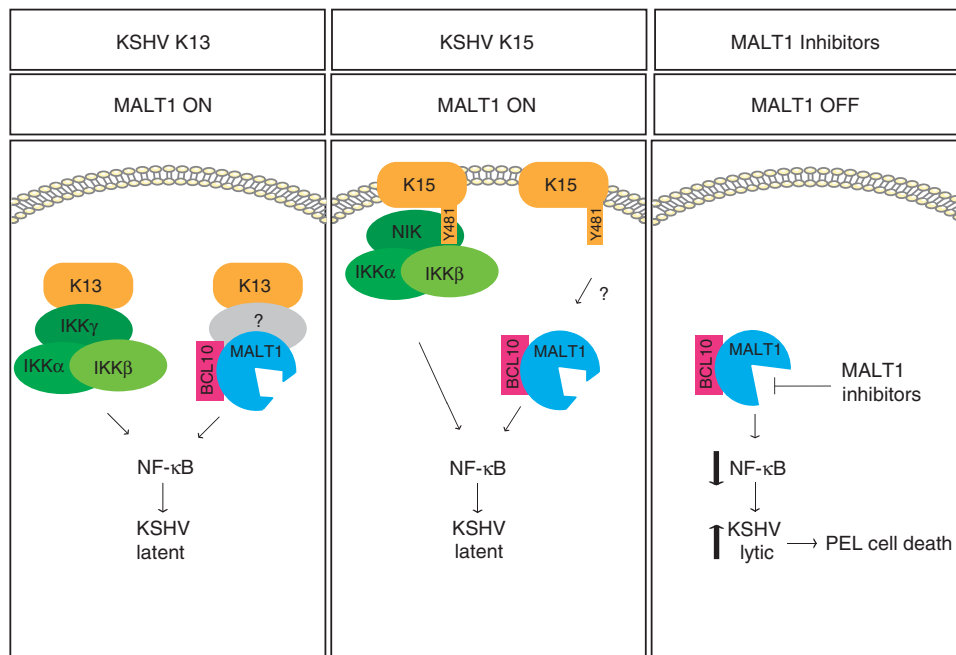


**Figure 8.** Model summarizing the proposed role of MALT1 in K13- and K15-mediated NF- $\kappa$ B activation and maintenance of viral latency. K13 promotes MALT1 activation by a direct or indirect interaction with its protease domain, whereas K15-dependent MALT1 activation may depend on the recruitment of an unknown signaling protein through Y481 in its cytoplasmic domain. Whether MALT1 and IKK components are part of the same or distinct K13-/K15-induced signaling complexes, and whether IKK- and MALT1-dependent NF- $\kappa$ B activation by K13 and K15 happens in a simultaneous or sequential manner remains unclear. Treatment of PEL cell lines with MALT1 inhibitors induces a switch from the latent to the lytic state of viral infection by impairment of MALT1-dependent NF- $\kappa$ B activation, which promotes lytic cell death of primary effusion lymphoma cells.

components are part of the same or distinct K13-/K15-induced signaling complexes, and whether IKK- and MALT1-dependent NF- $\kappa$ B activation by K13 and K15 happens in a simultaneous or sequential manner will have to be investigated in future studies.

Several different types of lymphomas are driven by oncogenic activation of the NF- $\kappa$ B pathway; signaling components driving NF- $\kappa$ B activation in tumor cells have thus gained attention as rational drug targets in lymphomas.<sup>29</sup> A lymphoma type with constitutive MALT1-dependent NF- $\kappa$ B activation is the ABC DLBCL, in which MALT1 is activated by chronic BCR-BTK-CARMA1 signaling.<sup>29</sup> The majority of ABC DLBCL cell lines therefore respond to inhibition of BCR signaling by the BTK inhibitor ibrutinib.<sup>29</sup> In contrast, PEL cell lines lack significant surface BCR expression,<sup>48</sup> and are resistant to treatment with Dasatinib, which inhibits upstream tyrosine kinase activity.<sup>49</sup> This suggests that NF- $\kappa$ B activation in PEL does not rely on early BCR-signaling events, but rather on K13- and K15-mediated NF- $\kappa$ B activation that occurs in a BTK- and CARMA1-independent, but MALT1- and IKK-dependent manner. Inhibition of NF- $\kappa$ B activation by the IKK inhibitor Bay-11-7082 efficiently inhibits the development of xenografted PEL *in vivo*.<sup>9</sup> Drugs targeting IKK-dependent NF- $\kappa$ B activation directly (such as IKK inhibitors) or indirectly (such as proteasome inhibitors) are under development or used in preclinical trials for PEL treatment,<sup>9,50</sup> but adverse side-effects of these drugs due to systemic NF- $\kappa$ B inhibition in all cell types and/or NF- $\kappa$ B independent effects of proteasome inhibitors remain a concern.<sup>51,52</sup> MALT1 activity, which appears to be important mainly for immune cells,<sup>53–56</sup> might thus be a rational alternative target for the treatment of PEL. Possible adverse side-effects of long-term MALT1 inhibition include compromised regulatory T cells responses and autoimmunity as MALT1 is required during embryonic development for the generation of regulatory T cells.<sup>53–56</sup> However, such side-effects have thus far not been reported during short-term treatments with MALT1 inhibitors. Our data using PEL cell lines and a xenograft model suggest that MALT1 inhibition may be efficient in purging the reservoir of latently infected PEL cells, promoting viral lytic replication. Therapeutic MALT1 inhibition should thus be combined with an anti-herpes virus drug that limits viral replication and spreading, such as the nucleoside analog ganciclovir.<sup>5,57</sup>

## CONFLICT OF INTEREST

The authors declare no conflict of interest.

## ACKNOWLEDGEMENTS

We would like to thank Mélanie Juilland and Mikhail Kuravsky for comments on the manuscript, Patrick Holz for technical advice and Elisa Oricchio for the kind gift of an antibody. This work was supported by grants from the Swiss National Science Foundation (SNSF), the Swiss Cancer League (KFS-02561-02-2010), the Helmut Horten Foundation and the Stiftung zur Krebsbekämpfung (to M Tho), by a DOD Career Development Award (CA140437 to ZQ), by a grant from the Leukemia Research Foundation (2016–2017 to ZQ), by the National Natural Science Foundation of China (81272191, 81472547, 81672924 to ZQ and 81400164 to LD), and by grants from the German Research Foundation (DFG: SFB 796, sub-project B9), the emerging fields initiative of the FAU Erlangen, and from the Interdisciplinary Center for Clinical Research (IZKF) of the Clinical Center Erlangen (to MS).

## REFERENCES

- Okada S, Goto H, Yotsumoto M. Current status of treatment for primary effusion lymphoma. *Intractable Rare Dis Res* 2014; **3**: 65–74.
- Schulz TF, Cesarman E. Kaposi Sarcoma-associated Herpesvirus: mechanisms of oncogenesis. *Curr Opin Virol* 2015; **14**: 116–128.
- Andrei G, Snoeck R. Kaposi's sarcoma-associated herpesvirus: the role of lytic replication in targeted therapy. *Curr Opin Infect Dis* 2015; **28**: 611–624.
- Klass CM, Krug LT, Pozharskaya VP, Offermann MK. The targeting of primary effusion lymphoma cells for apoptosis by inducing lytic replication of human herpesvirus 8 while blocking virus production. *Blood* 2005; **105**: 4028–4034.
- Kedes DH, Ganem D. Sensitivity of Kaposi's sarcoma-associated herpesvirus replication to antiviral drugs. Implications for potential therapy. *J Clin Invest* 1997; **99**: 2082–2086.
- Keller SA, Schattner EJ, Cesarman E. Inhibition of NF- $\kappa$ B induces apoptosis of KSHV-infected primary effusion lymphoma cells. *Blood* 2000; **96**: 2537–2542.
- Brown HJ, Song MJ, Deng H, Wu TT, Cheng G, Sun R. NF- $\kappa$ B inhibits gammaherpesvirus lytic replication. *J Virol* 2003; **77**: 8532–8540.
- Grossmann C, Ganem D. Effects of NF- $\kappa$ B activation on KSHV latency and lytic reactivation are complex and context-dependent. *Virology* 2008; **375**: 94–102.
- Keller SA, Hernandez-Hopkins D, Vider J, Ponomarev V, Hyjek E, Schattner EJ et al. NF- $\kappa$ B is essential for the progression of KSHV- and EBV-infected lymphomas *in vivo*. *Blood* 2006; **107**: 3295–3302.
- Krug LT, Moser JM, Dickerson SM, Speck SH. Inhibition of NF- $\kappa$ B activation *in vivo* impairs establishment of gammaherpesvirus latency. *PLoS Pathog* 2007; **3**: e11.
- Chaudhary PM, Jasmin A, Eby MT, Hood L. Modulation of the NF- $\kappa$ B pathway by virally encoded death effector domains-containing proteins. *Oncogene* 1999; **18**: 5738–5746.
- Brinkmann MM, Glenn M, Rainbow L, Kieser A, Henke-Gendo C, Schulz TF. Activation of mitogen-activated protein kinase and NF- $\kappa$ B pathways by a Kaposi's sarcoma-associated herpesvirus K15 membrane protein. *J Virol* 2003; **77**: 9346–9358.
- Steinbruck L, Gustems M, Medele S, Schulz TF, Lutter D, Hammerschmidt W. K1 and K15 of Kaposi's sarcoma-associated herpesvirus are partial functional homologues of latent membrane protein 2 A of Epstein-Barr virus. *J Virol* 2015; **89**: 7248–7261.
- Damania B. Oncogenic gamma-herpesviruses: comparison of viral proteins involved in tumorigenesis. *Nat Rev Microbiol* 2004; **2**: 656–668.
- Guasparri I, Keller SA, Cesarman E. KSHV vFLIP is essential for the survival of infected lymphoma cells. *J Exp Med* 2004; **199**: 993–1003.
- Sharp TV, Wang HW, Koumi A, Hollyman D, Endo Y, Ye H et al. K15 protein of Kaposi's sarcoma-associated herpesvirus is latently expressed and binds to HAX-1, a protein with antiapoptotic function. *J Virol* 2002; **76**: 802–816.
- Liu L, Eby MT, Rathore N, Sinha SK, Kumar A, Chaudhary PM. The human herpes virus 8-encoded viral FLICE inhibitory protein physically associates with and persistently activates the I $\kappa$ B kinase complex. *J Biol Chem* 2002; **277**: 13745–13751.
- Field N, Low W, Daniels M, Howell S, Daviet L, Boshoff C et al. KSHV vFLIP binds to IKK- $\gamma$  to activate IKK. *J Cell Sci* 2003; **116**: 3721–3728.
- Havemeier A, Gramolelli S, Pietrek M, Jochmann R, Sturz M, Schulz TF. Activation of NF- $\kappa$ B by the Kaposi's sarcoma-associated herpesvirus K15 protein involves recruitment of the NF- $\kappa$ B-inducing kinase, I $\kappa$ B kinases, and phosphorylation of p65. *J Virol* 2014; **88**: 13161–13172.
- Oeckinghaus A, Wegener E, Welteke V, Ferch U, Arslan SC, Ruland J et al. Malt1 ubiquitination triggers NF- $\kappa$ B signaling upon T-cell activation. *EMBO J* 2007; **26**: 4634–4645.
- Yang Y, Schmitz R, Mitala J, Whiting A, Xiao W, Ceribelli M et al. Essential role of the linear ubiquitin chain assembly complex in lymphoma revealed by rare germline polymorphisms. *Cancer Discov* 2014; **4**: 480–493.
- Dubois SM, Alexia C, Wu Y, Leclair HM, Leveau C, Schol E et al. A catalytic-independent role for the LUBAC in NF- $\kappa$ B activation upon antigen receptor engagement and in lymphoma cells. *Blood* 2014; **123**: 2199–2203.
- Coornaert B, Baens M, Heyninck K, Bekaert T, Haegman M, Staal J et al. T cell antigen receptor stimulation induces MALT1 paracaspase-mediated cleavage of the NF- $\kappa$ B inhibitor A20. *Nat Immunol* 2008; **9**: 263–271.
- Hailfinger S, Nogai H, Pelzer C, Jaworski M, Cabalzar K, Charton JE et al. Malt1-dependent RelB cleavage promotes canonical NF- $\kappa$ B activation in lymphocytes and lymphoma cell lines. *Proc Natl Acad Sci USA* 2011; **108**: 14596–14601.
- Rosebeck S, Rehman AO, Lucas PC, McAllister-Lucas LM. From MALT lymphoma to the CBM signalosome: three decades of discovery. *Cell Cycle* 2011; **10**: 2485–2496.
- Jaworski M, Thome M. The paracaspase MALT1: biological function and potential for therapeutic inhibition. *Cell Mol Life Sci* 2016; **73**: 459–473.
- Hailfinger S, Lenz G, Ngo V, Posvitz-Fejfar A, Rebeaud F, Guzzardi M et al. Essential role of MALT1 protease activity in activated B cell-like diffuse large B-cell lymphoma. *Proc Natl Acad Sci USA* 2009; **106**: 19946–19951.
- Ferch U, Kloob B, Gewies A, Pfander V, Duwel M, Peschel C et al. Inhibition of MALT1 protease activity is selectively toxic for activated B cell-like diffuse large B cell lymphoma cells. *J Exp Med* 2009; **206**: 2313–2320.
- Roschewski M, Staudt LM, Wilson WH. Diffuse large B-cell lymphoma-treatment approaches in the molecular era. *Nat Rev Clin Oncol* 2014; **11**: 12–23.

- 30 Nagel D, Spranger S, Vincendeau M, Grau M, Raffegerst S, Kloos B et al. Pharmacologic inhibition of MALT1 protease by phenothiazines as a therapeutic approach for the treatment of aggressive ABC-DLBCL. *Cancer Cell* 2012; **22**: 825–837.
- 31 Fontan L, Yang C, Kabaleeswaran V, Volpon L, Osborne MJ, Beltran E et al. MALT1 small molecule inhibitors specifically suppress ABC-DLBCL in vitro and in vivo. *Cancer Cell* 2012; **22**: 812–824.
- 32 Yoo SM, Zhou FC, Ye FC, Pan HY, Gao SJ. Early and sustained expression of latent and host modulating genes in coordinated transcriptional program of KSHV productive primary infection of human primary endothelial cells. *Virology* 2005; **343**: 47–64.
- 33 Vieira J, O'Hearn PM. Use of the red fluorescent protein as a marker of Kaposi's sarcoma-associated herpesvirus lytic gene expression. *Virology* 2004; **325**: 225–240.
- 34 Rebeaud F, Hailfinger S, Posevitz-Fejfar A, Tapernoux M, Moser R, Rueda D et al. The proteolytic activity of the paracaspase MALT1 is key in T cell activation. *Nat Immunol* 2008; **9**: 272–281.
- 35 Sander G, Konrad A, Thurau M, Wies E, Leubert R, Kremmer E et al. Intracellular localization map of human herpesvirus 8 proteins. *J Virol* 2008; **82**: 1908–1922.
- 36 Chudasama P, Konrad A, Jochmann R, Lausen B, Holz P, Naschberger E et al. Structural proteins of Kaposi's sarcoma-associated herpesvirus antagonize p53-mediated apoptosis. *Oncogene* 2015; **34**: 639–649.
- 37 Wu JJ, Li W, Shao Y, Avey D, Fu B, Gillen J et al. Inhibition of cGAS DNA sensing by a herpesvirus virion protein. *Cell Host Microbe* 2015; **18**: 333–344.
- 38 Rueda D, Gaide O, Ho L, Lewkowicz E, Niedergang F, Hailfinger S et al. Bcl10 controls TCR- and FcγR-induced actin polymerization. *J Immunol* 2007; **178**: 4373–4384.
- 39 Pelzer C, Cabalzar K, Wolf A, Gonzalez M, Lenz G, Thome M. The protease activity of the paracaspase MALT1 is controlled by monoubiquitination. *Nat Immunol* 2013; **14**: 337–345.
- 40 Ngo VN, Davis RE, Lamy L, Yu X, Zhao H, Lenz G et al. A loss-of-function RNA interference screen for molecular targets in cancer. *Nature* 2006; **441**: 106–110.
- 41 Dai L, Trillo-Tinoco J, Bai L, Kang B, Xu Z, Wen X et al. Systematic analysis of a xenograft mice model for KSHV+ primary effusion lymphoma (PEL). *PLoS One* 2014; **9**: e90349.
- 42 Baens M, Bonsignore L, Somers R, Vanderheydt C, Weeks SD, Gunnarsson J et al. MALT1 auto-proteolysis is essential for NF-κB-dependent gene transcription in activated lymphocytes. *PLoS One* 2014; **9**: e103774.
- 43 Gaide O, Favier B, Legler DF, Bonnet D, Brissoni B, Valitutti S et al. CARMA1 is a critical lipid raft-associated regulator of TCR-induced NF-κB activation. *Nat Immunol* 2002; **3**: 836–843.
- 44 Wang D, You Y, Case SM, McAllister-Lucas LM, Wang L, DiStefano PS et al. A requirement for CARMA1 in TCR-induced NF-κB activation. *Nat Immunol* 2002; **3**: 830–835.
- 45 de Oliveira DE, Ballon G, Cesarman E. NF-κB signaling modulation by EBV and KSHV. *Trends Microbiol* 2010; **18**: 248–257.
- 46 Guasparri I, Wu H, Cesarman E. The KSHV oncoprotein vFLIP contains a TRAF-interacting motif and requires TRAF2 and TRAF3 for signalling. *EMBO Rep* 2006; **7**: 114–119.
- 47 Sun L, Deng L, Ea CK, Xia ZP, Chen ZJ. The TRAF6 ubiquitin ligase and TAK1 kinase mediate IKK activation by BCL10 and MALT1 in T lymphocytes. *Mol Cell* 2004; **14**: 289–301.
- 48 Drexler HG, Uphoff CC, Gaidano G, Carbone A. Lymphoma cell lines: in vitro models for the study of HHV-8+ primary effusion lymphomas (body cavity-based lymphomas). *Leukemia* 1998; **12**: 1507–1517.
- 49 Lu P, Yang C, Guasparri I, Harrington W, Wang YL, Cesarman E. Early events of B-cell receptor signaling are not essential for the proliferation and viability of AIDS-related lymphoma. *Leukemia* 2009; **23**: 807–810.
- 50 Sarosiek KA, Cavallin LE, Bhatt S, Toomey NL, Natkunam Y, Blasini W et al. Efficacy of bortezomib in a direct xenograft model of primary effusion lymphoma. *Proc Natl Acad Sci USA* 2010; **107**: 13069–13074.
- 51 Baud V, Karin M. Is NF-κB a good target for cancer therapy? Hopes and pitfalls. *Nat Rev Drug Discov* 2009; **8**: 33–40.
- 52 Wang W, Nag SA, Zhang R. Targeting the NFκB signaling pathways for breast cancer prevention and therapy. *Curr Med Chem* 2015; **22**: 264–289.
- 53 Jaworski M, Marsland BJ, Gehrig J, Held W, Favre S, Luther SA et al. Malt1 protease inactivation efficiently dampens immune responses but causes spontaneous autoimmunity. *EMBO J* 2014; **33**: 2765–2781.
- 54 Bornancin F, Renner F, Touil R, Sic H, Kolb Y, Touil-Allaoui I et al. Deficiency of MALT1 paracaspase activity results in unbalanced regulatory and effector T and B cell responses leading to multiorgan inflammation. *J Immunol* 2015; **194**: 3723–3734.
- 55 Gewies A, Gorka O, Bergmann H, Pechloff K, Petermann F, Jeltsch KM et al. Uncoupling Malt1 threshold function from paracaspase activity results in destructive autoimmune inflammation. *Cell Rep* 2014; **9**: 1292–1305.
- 56 Yu JW, Hoffman S, Beal AM, Dykon A, Ringenberg MA, Hughes AC et al. MALT1 protease activity is required for innate and adaptive immune responses. *PLoS One* 2015; **10**: e0127083.
- 57 Klass CM, Offermann MK. Targeting human herpesvirus-8 for treatment of Kaposi's sarcoma and primary effusion lymphoma. *Curr Opin Oncol* 2005; **17**: 447–455.



This work is licensed under a Creative Commons Attribution-NonCommercial-NoDerivs 4.0 International License. The images or other third party material in this article are included in the article's Creative Commons license, unless indicated otherwise in the credit line; if the material is not included under the Creative Commons license, users will need to obtain permission from the license holder to reproduce the material. To view a copy of this license, visit <http://creativecommons.org/licenses/by-nc-nd/4.0/>

© The Author(s) 2017

Supplementary Information accompanies this paper on the Leukemia website (<http://www.nature.com/leu>)